Supporting Information

Exploring Reactive Conformations of Coenzyme A during Binding and Unbinding to Pyruvate Formate-Lyase

Marko Hanževački,[†,‡] Radha Dilip Banhatti,[†] Karmen Čondić-Jurkić,[†,§] Ana-Sunčana Smith,[†,‡] and David M. Smith[*,†]

[†]Group for Computational Life Sciences, Division for Physical Chemistry, Ruđer Bošković Institute, Bijenička cesta 54, 10000 Zagreb, Croatia

[‡]PULS Group, Department of Physics, Interdisciplinary Center for Nanostructured Films, Friedrich-Alexander-Universität Erlangen-Nürnberg, Cauerstraße 3, 91058 Erlangen, Germany

[§]Memorial Sloan Kettering Cancer Center, New York, New York 10065, United States

[*]Corresponding author e-mail: david.smith@irb.hr

Table of Contents:

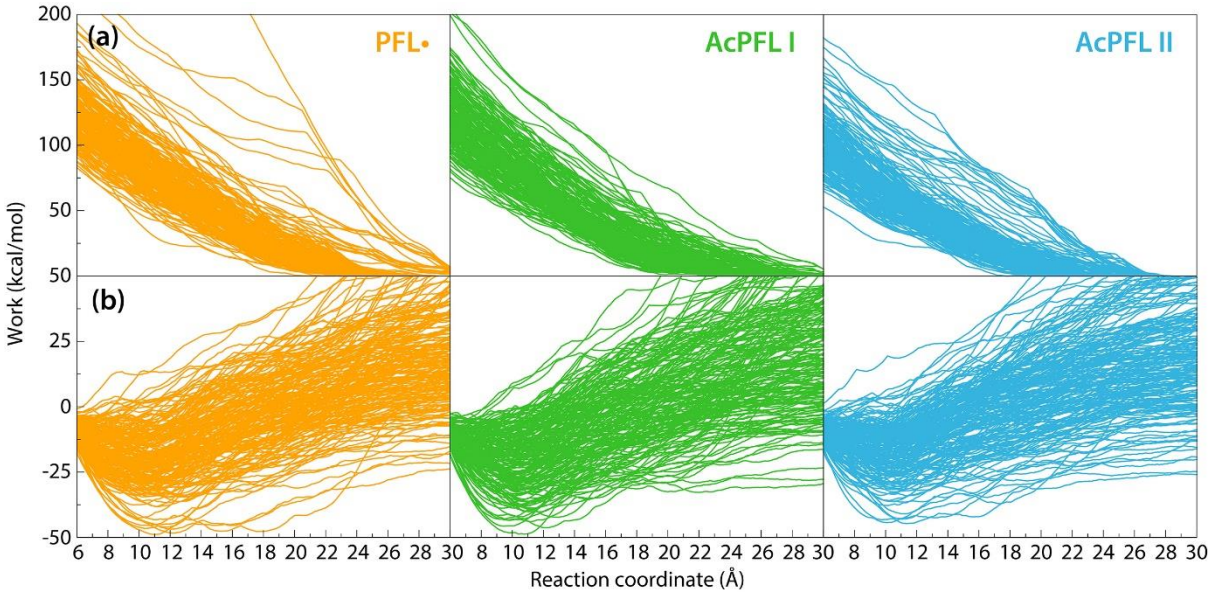

Figure S1 Trajectories obtained from the SMD simulations in which CoA is pulled towards (forward) and away (reverse) from the active site before (**PFL•**) and after (**AcPFL I** and **AcPFL II**) the first half–reaction. The smooth lines represent the amount of work as a function of the values of the RC for each of the two hundred runs during the (a) forward and (b) reverse pulling "experiments".

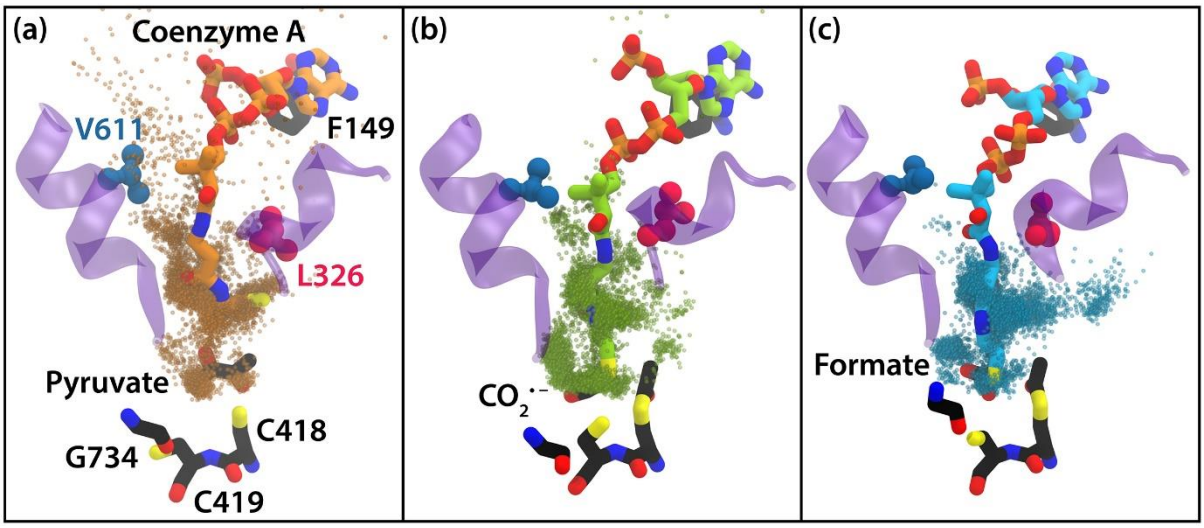

Figure S2 Ensemble of S-atom of CoA cysteamine moiety (shown as transparent spheres) derived from unrestrained MD starting from 150 final snapshots taken after forward pulls in both non-acetylated (**PFL•**) and acetylated (**AcPFL I** and **AcPFL II**) systems. In these simulations CoA was left to explore the channel from the active site to the protein surface through the L-V gate. Panels (a), (b) and (c) are showing the CoA tail S-atom occupation of the certain regions in the channel in **PFL•** (orange), **AcPFL I** (green) and **AcPFL II** (blue) model systems, respectively.

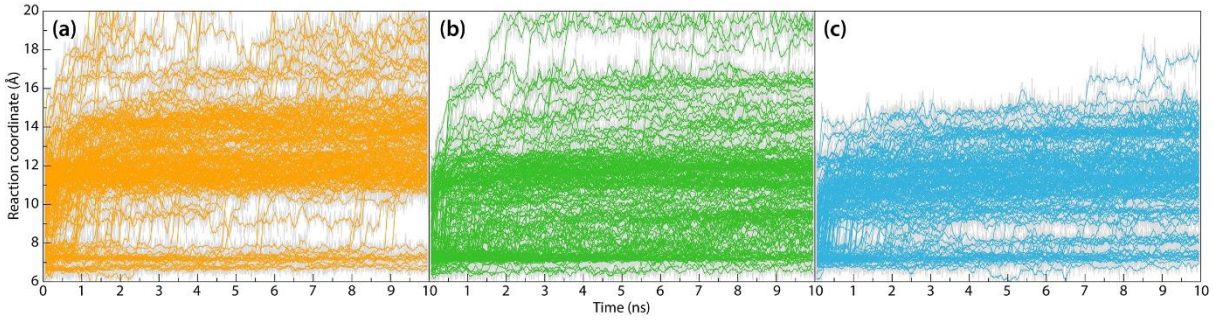

Figure S3 Time traces of distance between groups of atoms defining a reaction coordinate over the duration (10 ns) of unrestrained MD simulations of the initial bound states starting from 150 final snapshots obtained with forward pulls in (a) **PFL•**, (b) **AcPFL I** and (c) **AcPFL II** systems.

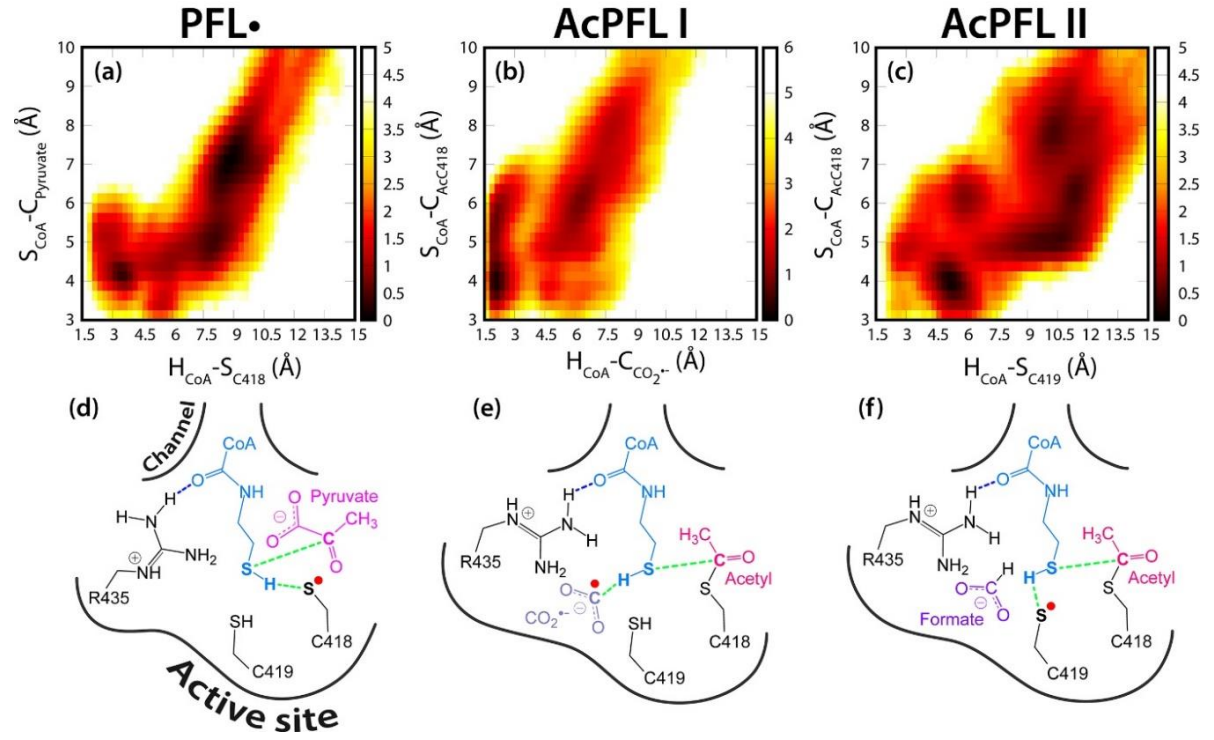

Figure S4 To construct heatmaps in panels (a), (b) and (c) the snapshots were taken from both non-acetylated (**PFL•**) and acetylated (**AcPFL I** and **AcPFL II**) systems, respectively. The geometrical parameters were monitored, namely H-abstraction coordinate (x-axis) distances were plotted against CoA-acetylation coordinate (y-axis) distances. The heatmap surface is given by $G_i = -k_BT \ln (N_i/N_{tot})$, where k_B is Boltzmann's constant, T is the temperature (300 K), N_i is the population of bin i while N_{tot} represents the total number of configurations of each system (N_{tot} is 150 000 for each system). The rightmost scale in the panels (a), (b) and (c) corresponds to relative free energy in kcal/mol obtained by counting the structures in each bin for each of our three model systems, respectively. Panels (d), (e) and (f) are showing 2D representative structures of CoA interacting with the residues in the active site of the non-acetylated (**PFL•**) and acetylated (**AcPFL I** and **AcPFL II**) systems, respectively. The location of the radical in each model system is denoted by the symbol '•'. These 2D structures of CoA bound in the active site of PFL show the important contacts of CoA with the active site compartments in each model system and are also depicted in the zoomed part in the lower panels of **Figures 5c-e** of the corresponding manuscript, where more structural details are provided.

Full Citations for References 25, 52 and 56

25. Wang, L.; Wu, Y.; Deng, Y.; Kim, B.; Pierce, L.; Krilov, G.; Lupyan, D.; Robinson S.; Dahlgren, M .K.; Greenwood, J.; Romero, D. L.; Masse, C.; Knight, J. L.; Steinbrecher, T.; Beuming, T.; Damm, W.; Harder, E.; Sherman, W.; Brewer, M.; Wester, R.; Murcko, M.; Frye, L.; Farid, R.; Lin, T.; Mobley, D. L.; Jorgensen, W. L.; Berne, B. J.; Friesner, R. A.; Abel, R. Accurate and Reliable Prediction of Relative Ligand Binding Potency in Prospective Drug Discovery by Way of a Modern Free-Energy Calculation Protocol and Force Field. *J. Am. Chem. Soc.* **2015**, *137*, 2695-2703.

52. Chovancova, E.; Pavelka, A.; Benes, P.; Strnad, O.; Brezovsky, J.; Kozlikova, B.; Gora, A.; Sustr, V.; Klvana, M.; Medek, P.; Biedermannova, L.; Sochor, J.; Damborsky, J. CAVER 3.0: A Tool for the Analysis of Transport Pathways in Dynamic Protein Structures. *PLoS Comput. Biol.* **2012**, *8*, e1002708.

56. Case, D. A.; Cerutti, D. S.; Cheatham, T. E., III; Darden, T. A.; Duke, R. E.; Giese, T. J.; Gohlke, H.; Goetz, A. W.; Greene, D.; Homeyer, N.; Izadi, S.; Kovalenko, A.; Lee, T. S.; LeGrand, S.; Li, P.; Lin, C.; Liu, J.; Luchko, T.; Luo, R.; Mermelstein, D.; Merz, K. M.; Monard, G.; Nguyen, H.; Omelyan, I.; Onufriev, A.; Pan, F.; Qi, R.; Roe, D. R.; Roitberg, A.; Sagui, C.; Simmerling, C. L.; Botello-Smith, W.-M.; Swails, J.; Walker, R. C.; Wang, J.; Wolf, R. M.; Wu, X.; Xiao, L.; York, D. M.; Kollman, P. A. AMBER 2017, University of California: San Francisco, CA, 2017.